Directed *d*-mer diffusion describing the Kardar-Parisi-Zhang-type surface growth

Géza Ódor,[1] Bartosz Liedke,[2] and Karl-Heinz Heinig[2]

[1]*Research Institute for Technical Physics and Materials Science, P.O. Box 49, H-1525 Budapest, Hungary*
[2]*Institute of Ion Beam Physics and Materials Research, Forschungszentrum Dresden-Rossendorf, P.O. Box 51 01 19, 01314 Dresden, Germany*

We show that $d+1$-dimensional surface growth models can be mapped onto driven lattice gases of d-mers. The continuous surface growth corresponds to one dimensional drift of d-mers perpendicular to the $(d-1)$-dimensional "plane" spanned by the d-mers. This facilitates efficient bit-coded algorithms with generalized Kawasaki dynamics of spins. Our simulations in $d=2$, 3, 4, 5 dimensions provide scaling exponent estimates on much larger system sizes and simulations times published so far, where the effective growth exponent exhibits an increase. We provide evidence for the agreement with field theoretical predictions of the Kardar-Parisi-Zhang universality class and numerical results. We show that the $(2+1)$-dimensional exponents conciliate with the values suggested by Lässig within error margin, for the largest system sizes studied here, but we cannot support his predictions for $(3+1)d$ numerically.

One of the simplest nonlinear stochastic differential equation set up by Kardar, Parisi, and Zhang (KPZ) [1] describes the dynamics of growth processes in the thermodynamic limit. It specifies the evolution of the height function $h(\mathbf{x},t)$ in the d-dimensional space

$$\partial_t h(\mathbf{x},t) = v + \sigma\nabla^2 h(\mathbf{x},t) + \lambda[\nabla h(\mathbf{x},t)]^2 + \eta(\mathbf{x},t). \quad (1)$$

Here v and λ are the amplitudes of the mean and local growth velocity, σ is a smoothing surface tension coefficient, and η roughens the surface by a zero-average Gaussian noise field exhibiting the variance $\langle\eta(\mathbf{x},t)\eta(\mathbf{x}',t')\rangle = 2D\delta^d(\mathbf{x}-\mathbf{x}')(t-t')$. The notation D is used for the noise amplitude and $\langle\ \rangle$ means the distribution average.

The KPZ equation was inspired in part by the stochastic Burgers equation [2], which belongs to the same universality class [3], and it became the subject of many theoretical studies [4–6]. Besides, it models other important physical phenomena such as directed polymers [7], randomly stirred fluid [3], dissipative transport [8,9], and the magnetic flux lines in superconductors [10]. The equation is solvable in $(1+1)d$ [11], but in higher dimensions approximations are available only. As the result of the competition of roughening and smoothing terms, models described by the KPZ equation exhibit a roughening phase transition between a weak-coupling regime $(\lambda < \lambda_c)$, governed by the Edwards-Wilkinson (EW) fixed point at $\lambda=0$ [12], and a strong-coupling phase. The strong-coupling fixed point is inaccessible by perturbative renormalization-group (RG) method. Therefore, the KPZ phase space has been the subject of controversies and the value of the upper critical dimension has been debated for a long time.

Using a directed polymer representation, the validity of a scaling hypothesis [13] and the two-loop RG calculation for $d \geq 2$ [14] was confirmed and extended to all orders in $d = (2+\epsilon)$ [15]. These results provided an argument for an upper critical dimension $d_c=4$ of the roughening transition, but the strong-coupling rough phase is not accessible by perturbation theory. Above $d=1$ the scaling behavior in the rough phase has been very controversial, diverse values for the

scaling exponents were claimed [16–18]. In particular, assuming that height correlations exhibit no multiscaling and satisfy an operator product expansion, exact field-theoretic methods lead to rational number growth values in two and three dimensions [17]. Some theoretical approaches predict that $d_c=4$ is an upper critical dimension of the rough phase [19–22]. Recently, a nonperturbative RG study has been able to describe the strong-coupling fixed point and has provided indications for a possible qualitative change in the critical behavior around $d=4$ [23]. This is in contradiction with the numerical results [24–27], which predict the lack of an upper critical dimension.

Mapping of surface growth onto reaction-diffusion system allow effective numerical simulations [28,29]. As a generalization of the $1+1$ dimensional roof-top model [30,31] and the $2+1$ dimensional octahedron model [32], we consider the deposition and removal processes of higher dimensional objects on $d \geq 2$ dimensional surfaces. We remind that in $1+1$ dimensions a continuous surface line having no overhangs can be approximated by $45°$ up/down slope elements (after appropriate length rescaling). A process with KPZ scaling can be realized by deposition at local minima or removal of local maxima (roof top). If we associate the up slopes with "particles" and down slopes with "holes" of the base lattice [see Fig. 1(a)], the adsorption or desorption corresponds to the asymmetric exclusion process (ASEP) [33]. This is a lattice gas [34,35], where particles can hop on adjacent sites with asymmetric rates and hardcore exclusion. Its behavior is well known, and variations in ASEP (disorder, interactions, etc.) correspond to variations in $1+1$-dimensional KPZ growth models.

We have extended the roof-top construction to $(2+1)$ dimensions [32] by the introduction of octahedra having four slopes. The up edges in the x or y directions can be represented by "+1," while the down ones by "−1," and a surface element update is a generalized (Kawasaki) exchange [Eq. (3) of [32]]. The translation of up edges to particles and the down ones to holes of the base lattice maps particle deposition or removal processes onto two simultaneous particle moves (one in the x and one in the y direction). One can also
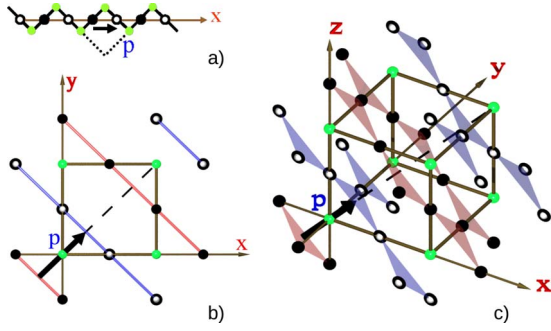
FIG. 1. (Color online) Mapping of (a) one-, (b) two-, (c) three-dimensional surface growth (discrete up/down derivatives) onto 1,2,3-dimensional oriented motion of d-mers. In general a deposition event corresponds to a d-Kawasaki exchange or a d-mer hopping in the bisectrix direction of axes. Up and down slopes between lattice points (pale green dots at the line corners) are denoted by full and empty circles, corresponding to particles/holes on the projection space. The surface continuity translates into particle exclusion, which makes the model nontrivial in higher dimensions.

consider it as a dimer move in the bisectrix directions of x and y [see Fig. 1(b)]. Therefore, the $(2+1)$ surface dynamics can be mapped onto a "two-dimensional ASEP" of oriented dimers exhibiting hardcore exclusion. The asymmetric drift corresponds to an evolving surface exhibiting KPZ scaling, while the symmetric dimer diffusion is related to the EW behavior.

Now we proceed with this kind of construction, considering the discrete slope variables in higher dimensions and generalize the simultaneous $+1 \leftrightarrow -1$ (Kawasaki) exchange rule of them [Eq. (3) of [32]] to d-dimensional updates

$$
\begin{pmatrix} -1 & 1 \\ -1 & 1 \\ -1 & 1 \\ \dots \end{pmatrix} \overset{p}{\underset{q}{\rightleftharpoons}} \begin{pmatrix} 1 & -1 \\ 1 & -1 \\ 1 & -1 \\ \dots \end{pmatrix}, \tag{2}
$$

with probability p for attachment and probability q for detachment [see Fig. 1(c) for the 3d case]. It is well known [4] that the surface evolution of the deterministic KPZ growth are described also by the Burgers equation [2] for growth velocities $\mathbf{v}(\mathbf{x},t)$ in the surface normal obeying

$$
\partial_t \mathbf{v}(\mathbf{x},t) = \sigma \nabla^2 \mathbf{v}(\mathbf{x},t) + \lambda \mathbf{v}(\mathbf{x},t) \nabla \mathbf{v}(\mathbf{x},t) \tag{3}
$$

due to the transformation $\mathbf{v}(\mathbf{x},t) = \nabla h(\mathbf{x},t)$.

In the forthcoming part we will prove that our microscopic model for d-mers in the continuum limit can be mapped onto the anisotropic version of Eq. (3), similarly as shown in lower dimensions [31,32]. The derivation is based on the formulation of the reduction in possible updates. Our surface model is represented by the discrete derivative elements: δ_x, δ_y, δ_z, $\dots$,$(\in \pm 1)$ at every lattice points. A generalized Kawasaki update [Eq. (2)] is defined by a matrix

$$
\begin{pmatrix} \delta_x(i-1,j,k,\dots) & \delta_x(i,j,k,\dots) \\ \delta_y(i,j-1,k,\dots) & \delta_y(i,j,k,\dots) \\ \delta_z(i,j,k-1,\dots) & \delta_z(i,j,k,\dots) \\ \dots \end{pmatrix}. \tag{4}
$$

In d dimensions we define vectors of the slopes, the columns of Eq. (4), analogously to one and two dimensions: $\bar{\sigma}_{i,j,k,\dots} = [\delta_x(i-1,j,k,\dots), \delta_y(i,j-1,k,\dots),\dots]$, around the lattice point, which we select for deposition or removal update and set up a microscopic master equation

$$
\partial_t P(\{\bar{\sigma}\},t) = \sum_{i,j,k,\dots} w'_{i,j,k,\dots}(\{\bar{\sigma}\})P(\{\bar{\sigma}'\},t)
$$
$$
- \sum_{i,j,k,\dots} w_{i,j,k,\dots}(\{\bar{\sigma}\})P(\{\bar{\sigma}\},t), \tag{5}
$$

with the probability distribution $P(\{\bar{\sigma}\},t)$. Here the prime index denotes the state of $\bar{\sigma}$ following the update [Eq. (2)]. The transition probability of $\bar{\sigma}$-s can be expressed as

$$
w_{i,j,k,\dots}(\{\bar{\sigma}\}) = A[1 - \bar{\sigma}_{i+1,j+1,k+1,\dots}\bar{\sigma}_{i,j,k,\dots}
$$
$$
+ \lambda(\bar{\sigma}_{i+1,j+1,k+1,\dots} - \bar{\sigma}_{i,j,k,\dots})], \tag{6}
$$

with $\lambda = 2p/(p+q) - 1$ parametrization, which formally looks like the Kawasaki exchange probability in 1d, except the factor A, which is necessary to avoid surface discontinuity creation in higher dimensions. This means that we update the slope configurations only if the values of all coordinates of the vector $\bar{\sigma}$ are identical as shown by Eq. (2). One can allow formally these updates via the expression

$$
A = 1/2^{d+1} \det[(\bar{\sigma}_{i,j,k,\dots} + C\bar{\sigma}_{i,j,k,\dots})
$$
$$
\times (\bar{\sigma}_{i+1,j+1,k+1,\dots} + C\bar{\sigma}_{i+1,j+1,k+1,\dots})I], \tag{7}
$$

where I and C are the unity and the cyclic permutation matrices, respectively. The matrix C shifts each coordinate value to the next index value. Thus for $\bar{\sigma}$-s with mixed coordinate values, the vectors $(\bar{\sigma}_{i,j,k,\dots} + C\bar{\sigma}_{i,j,k,\dots}) = \bar{k}$ or $(\bar{\sigma}_{i+1,j+1,k+1,\dots} + C\bar{\sigma}_{i+1,j+1,k+1,\dots}) = \bar{k}'$ possess zero elements. Therefore the determinant of $\bar{k}\bar{k}'I$, being the product of the diagonal elements, is zero in case of mixed coordinates and $A = 1/2^{d+1}$ in case of equal coordinates.

For example a $d=3$ update is prohibited when the slope vector is $\bar{\sigma} = (1,1,-1)$ because $\bar{k}$ has one coordinate value of zero

$$
\bar{k} = \begin{pmatrix} 1 \\ 1 \\ -1 \end{pmatrix} + \begin{pmatrix} 0 & 1 & 0 \\ 0 & 0 & 1 \\ 1 & 0 & 0 \end{pmatrix} \begin{pmatrix} 1 \\ 1 \\ -1 \end{pmatrix} = \begin{pmatrix} 2 \\ 0 \\ -2 \end{pmatrix}.
$$

By calling $+1$s as particles and the -1s as holes of the base lattice, their synchronous update can be considered to be a single step motion of an oriented d-mer in the bisectrix direction of the x, y, z,... coordinate axes. Thus d-mers follow one-dimensional kinetics, described by Kawasaki exchanges [Eq. (6)]. To obtain a one-to-one mapping we update neighborhoods of the lattice points denoted by the green dots of Fig. 1.

To derive Eq. (3) first we have to average over the slope vectors

$$\langle \bar{\sigma} \rangle = \sum_{\{\bar{\sigma}\}} \bar{\sigma} P(\{\bar{\sigma}\}, t). \tag{8}$$

By calculating its time derivative using the master Eq. (5) and the transition probabilities [Eq. (6)]

$$\partial_t \langle \bar{\sigma} \rangle = \sum_{\{\bar{\sigma}\}} \left[\bar{\sigma} \sum_{i,j,k,\dots} w'_{i,j,k,\dots}(\{\bar{\sigma}\}) P(\{\bar{\sigma}'\}, t) \right.$$
$$\left. - \bar{\sigma} \sum_{i,j,k,\dots} w_{i,j,k,\dots}(\{\bar{\sigma}\}) P(\{\bar{\sigma}\}, t) \right], \tag{9}$$

in which we filter out vectors of nonequal coordinates [Eq. (7)] (thus $w_{i,j,k,\dots}$ is nonzero only if $\bar{\sigma}_{i,j,\dots} \neq \bar{\sigma}_{i+1,j+1,\dots}$), we can obtain

$$2\partial_t \langle \bar{\sigma}_{i,j,k,\dots} \rangle = \langle \bar{\sigma}_{i-1,j-1,\dots} \rangle - 2\langle \bar{\sigma}_{i,j,\dots} \rangle + \langle \bar{\sigma}_{i+1,j+1,\dots} \rangle$$
$$+ \lambda \langle \bar{\sigma}_{i,j}(\bar{\sigma}_{i+1,j+1,\dots} - \bar{\sigma}_{i-1,j-1,\dots}) \rangle, \tag{10}$$

analogously to one dimension [31]. Here one can see the discrete first and second differentials of $\bar{\sigma}_{i,j,k,\dots}$ corresponding to the operators of Eq. (3) in the bisectrix direction of the axes. These differentials are one-dimensional because the *d*-mer dynamics is one dimensional. In principle one could derive a set of coupled Burgers equations for the particles in each direction in an isotropic way in accordance with isotropic surface model, but the coordinated movements reduce the dimensionality and we can map onto an anisotropic equation of *d*-mers.

Making a continuum limit in each direction and taking into account the relation of height and slope variables $[\mathbf{v}(\mathbf{x},t) = \nabla h(\mathbf{x},t)]$, we can arrive to the deterministic KPZ equation. The nonlinear term vanishes for $p=q$ ($\lambda=0$). The sign of the coefficient λ of the nonlinear term can be interpreted as follows: for $p>q$ positive nonlinearity (positive excess velocity) it is a consequence of growth with voids.

Since this derivation was applied just for the first one in the hierarchy of equations for correlation functions it does not prove the equivalence to the stochastic KPZ. Furthermore, the form of the noise term, which was not considered in our derivation, may also introduce differences. Although our surface model is spatially isotropic, we can map it onto a one-dimensional Burgers equation (of extended objects), therefore anisotropic scaling behavior might be expected. However, by going into the continuum description the hardcore exclusions necessary to provide continuous surfaces is lost, and the resulting equation looks trivial.

Here we investigate by numerical simulations this isotopic surface growth model via the one-dimensional directed migration of *d*-mers in the *d*-dimensional space. We have developed bit-coded algorithms for the updates [Eq. (2)] and run it with $p=1$, such that randomness comes from the site selection only. Therefore it is important to use a very good random number generator, which provides uniformly distributed numbers with high resolution. Otherwise we would realize a process with quenched disorder, which for KPZ belongs to a different universality class (see [29]). We used the latest Mersenne-Twister generator [36] in general, which has

very good statistical properties and which is very fast, especially in the SSE2 registers. We tested our results using other random number generators as well. In practice each update site can be characterized by the 2^{d^2} different local slope configurations. However, due to the surface continuity we need only a few bits of a world (1 byte for $d=2$, 3, 4 and two bytes for $d=5$) for this purpose. This allows an efficient storage management in the computer memory and permits simulations of larger system sizes. The updates can be performed by logical operations, either on multiple samples at once or on multiple (not overlapping) sites at once. Our bit-coded algorithm proved to be ~ 40 times faster than the conventional FORTRAN 90 code we started with. It is important to note that this stochastic cellular automatonlike representation of the surface growth opens the possibility for an implementation on extremely fast graphic cards with massively parallel processors. Furthermore the construction permits the extension of the mapping for more complex surface reactions [37].

We performed dynamical simulations by starting from stripe-ordered particle distributions. This corresponds to a flat surface with a small intrinsic width. The considered lattices gases had the maximum linear sizes $L_{\max}=2^{15}$, 2^{10}, 2^8, 2^6 for $d=2$, 3, 4, 5 dimensions, respectively, and periodic boundary conditions were applied. A single step of the lattice gas algorithm comprises a random site selection and in case of an appropriate neighborhood configuration a $p=1$ Kawasaki *d*-mer update [Eq. (2)]. The time is incremented by $1/L^d$ in units of Monte Carlo steps (MCs). Throughout the paper we will use this unit of time.

We could exceed by magnitudes of order all previous numerical system sizes and simulation times. For example the largest five-dimensional simulations were done for $L=30$ and $t_m=230$ MCs [25]. Our $L=64$ simulations, where we have the good bulk/surface ratio: 5.4, required 2 GB memory size and a couple of weeks for a single realization up to $t_{\max}=5000$ MCs. Similarly, the largest sized simulations in $d=2$ for $L=11\,520$ system could achieve $t_{\max}=10^4$ MCs [38]. Our largest $L=32\,768$ sized simulations reached $t_{\max}=44\,600$ MCs. The longest runs for $L=4096$ passed the saturation at $t \simeq 4 \times 10^5$ MCs and the samples were followed up to $t_{\max}=10^6$ MCs.

We run the these lattice gas simulations for 10–1000 independent realizations for each dimension and size considered, and calculated $h_{x,y,\dots}(t)$ and the second moment

$$W(L,t) = \left[\frac{1}{L^{2d}} \sum_{x,y,\dots}^{L} h^2_{x,y,\dots}(t) - \left(\frac{1}{L^d} \sum_{x,y,\dots}^{L} h_{x,y,\dots}(t) \right)^2 \right]^{1/2} \tag{11}$$

from the height differences at certain sampling times. The growth is expected to follow the Family-Vicsek scaling [39] asymptotically, but due to the corrections it can be described by a power series

$$W(t, L \to \infty) = bt^\beta (1 + b_0 t^{\phi_0} + b_1 t^{\phi_1} \cdots), \tag{12}$$

with the surface growth exponent β. For finite system, when the correlation length exceeds L, the growth crosses over to a saturation with the scaling law

$$W(t \to \infty, L) = aL^\alpha (1 + a_0 L^{\omega_0} + a_1 L^{\omega_1} \cdots), \quad (13)$$

characterized by the roughness exponent α. In our case the intrinsic width of the initial state, which is represented by a zigzag surface of width 1/2 (see Fig. 1), results in a constant correction term. Thus we have $b_0 = 1/2$, $\phi_0 = -\beta$ and $a_0 = 1/2$, $\omega_0 = -\alpha$. During our scaling analysis we dropped this contribution by subtracting $W^2(0) = 1/4$ from the raw data and consider the next leading order correction as leading one. Furthermore we disregarded the initial time region $t < t_0 \simeq 50$ when basically an uncorrelated random deposition occurs. The dynamical exponent z can be expressed by the ratio $z = \alpha/\beta$ and in case of the Galilean invariance of an isotropic KPZ equation the $z = 2 - \alpha$ relation should also hold.

Besides the extensive simulations we have performed careful correction to scaling analysis by calculating the local slopes of the exponents. The effective exponent of the surface growth can be estimated similarly as in case of other scaling laws [29], as the discretized, logarithmic derivative of Eq. (11)

$$\beta_{eff}(t) = \frac{\ln W(t, L \to \infty) - \ln W(t', L \to \infty)}{\ln(t) - \ln(t')}. \quad (14)$$

It was determined numerically for different discretizations: $t/t' = 2, 3$, and we tried to fit it with the leading-order correction ansatz, which can easily be deduced from Eq. (12) (see [40] or [29])

$$\beta_{eff}(t) = \beta + b_1 \phi_1 t^{\phi_1}, \quad (15)$$

for $t > t_0$ and before the saturation region. In other cases, such as ballistic deposition, which has a large unknown intrinsic width one can use another effective roughness exponent definition introduced in [40].

We tested our method with the *one-dimensional* exactly known case. Simulations were run on $L = 5 \times 10^5$ sized system up to $t_{max} = 16\,666$ MCs for 40 independent realizations. We determined the effective exponents $\beta_{eff}(t)$, which approaches $\beta = 1/3$ from below, in a perfect agreement with the leading-order correction form (see Fig. 2). The fitting with Eq. (15) on the local slopes data resulted in $\beta = 0.333(5)$ and $\phi_1 = -0.53$.

Similarly to the time dependence we can analyze the size dependence following the saturation by determining the effective exponent of the roughness, which can be defined as the logarithmic derivative of Eq. (11)

$$\alpha_{eff}(L) = \frac{\ln W(t \to \infty, L) - \ln W(t \to \infty, L')}{\ln(L) - \ln(L')}. \quad (16)$$

The finite-size scaling was done for systems of linear sizes in between L_{max} (discussed earlier) and L_{min}, which was 2^6 for 2d, 2^5 for 3d, 2^4 for 4d, and 2^3 for 5d, respectively. To handle the boundary conditions effectively, system sizes of power of two were simulated. To get the asymptotic values we took into account all effective exponent points shown on Fig. 4 and applied a leading-order linear fitting. The error margins of exponents are estimated from the error bars of Fig. 4. This method gives a better estimate for the asymptotic values than just a least-square fitting on the data points, which completely disregards corrections to scaling. We also calculated
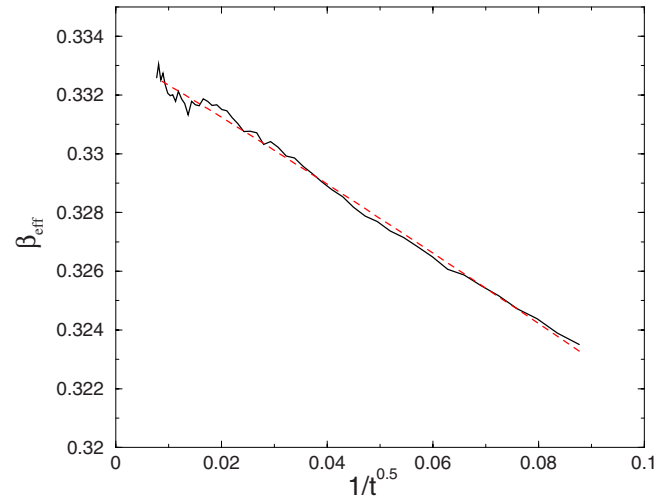

FIG. 2. (Color online) Effective exponents of the growth of the $d = 1$ dimensional model. The solid line corresponds to the simulation result. The dashed lines shows a fitting with form (15).

rough but independent estimates for z by measuring the relaxation time, i.e., the time needed to reach 90% of the saturation value. The asymptotic value is extrapolated by a linear fitting: $z_{eff}(t) = z + c_1/L$.

In *two dimensions* we estimated the growth exponent in the largest system sizes considered ($L = 2^{15}, 2^{14}, 2^{13}$) (see Fig. 3). Fitting in the $50 < t < 44\,600$ time window with form (15) resulted in $b_1 = 0.83$ and $\beta = 0.245(5)$, which is somewhat bigger than what was obtained by the largest known ($L = 11\,520$) sized simulations: $\beta = 0.240(1)$ [38], and all other previous numerical estimates including ours [32,40,41]. This value conciliates with the $\beta = 1/4$ RG exponent of [17]. One can obtain this value by the late time behavior of effective exponent, which has not been seen before, because finite-size
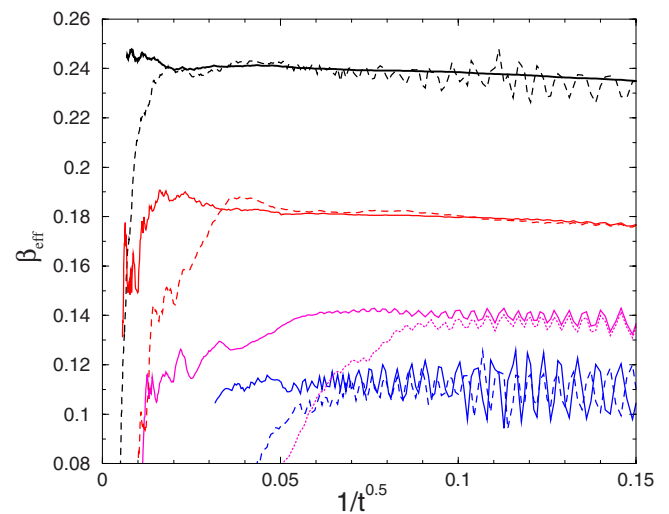

FIG. 3. (Color online) Effective exponents of the growth of the $d = 2, 3, 4, 5$ dimensional model (top to bottom). Solid lines correspond to the largest system $L = 2^{15}$, $L = 2^{10}$, $L = 2^8$, and $L = 2^6$, respectively. Dashed lines show our results of smaller sizes: $L = 2^{10}$, $L = 2^8$, $L = 2^5$, and $L = 2^5$, respectively, where saturation sets in earlier causing a cutoff in the scaling.
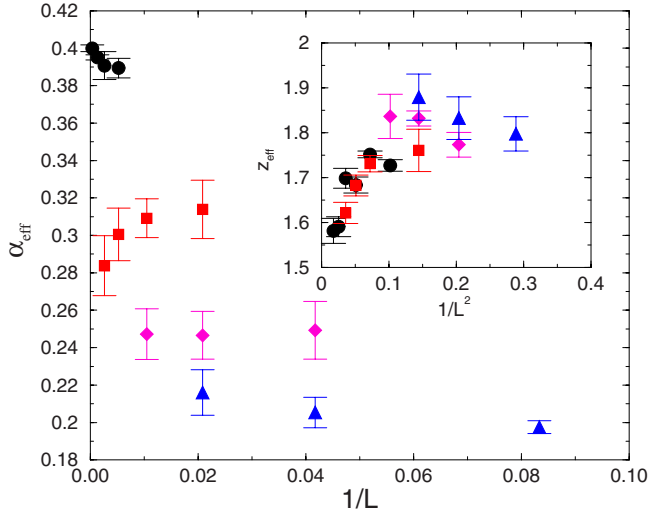
FIG. 4. (Color online) Local slopes of the finite-size scaling of the saturation width in $d=2$, 3, 4, 5 dimensions (top to bottom). Inset: effective exponents of the characteristic times.

effects have screened it. On the graph one can see strong oscillations for $L=2^{10}$ and intermediate times, which are damped before saturation. In the one-dimensional ASEP model such oscillations are shown to be the consequence of density fluctuations being transported through a finite system by kinematic waves [42]. One can speculate that the slight final increase in β_{eff} for the largest system sizes is just a fluctuation or oscillation effect, but we could not eliminate this overall tendency by increasing the statistics. Although the statistical fluctuations grow dramatically, as $t \to \infty$ the increase in the mean value is observable for each size $L > 2^{11}$. Our error bar of β reflects this uncertainty. The width saturation values have been investigated for $L = 2^6, 2^7, \ldots, 2^{12}$. We took into account the leading-order correction to scaling by the following ansatz:

$$\alpha_{eff}(L) = \alpha + a_1 \omega_1 L^{\omega_1}, \qquad (17)$$

but due to the larger error-bars we restricted it to a linear approximation: $\omega_1 = -1$. The local slopes of the steady state values $\alpha_{eff}(1/L)$ and of $z_{eff}(1/L)$ are shown on Fig. 4. This provides $\alpha=0.395(5)$ and $a_1=2.02$ for the roughness and $z_{eff}=1.58(10)$, with the linear coefficient $c_1=1.83$ for the dynamical exponent. This roughness exponent is in agreement with RG value [17], and somewhat bigger than the existing figures $\alpha=0.393(3)$ [26] for $L \leq 1024$ and $\alpha=0.385(5)$ [38] for $L \leq 128$.

In *three dimensions* the local slope analysis for $L=2^{10}$ results in $b_1=0.1$ and $\beta=0.184(5)$ agreeing with the numerical results from the literature: $\beta=0.180(2)$ [25,38] and $\beta=0.186(1)$ [26]. But our estimate is much higher than $\beta=0.168(3)$ [41] (based on $L<200$ sized simulations) and $\beta=1/6$ predicted by RG [17]. For the saturation we obtained $a_1=1.40$ and $\alpha=0.29(1)$, matching $\alpha=0.29$ of [41] and in marginal agreement with $\alpha=0.3135(15)$ of [26] and $\alpha=0.308(2)$ of [25]. The direct z_{eff} measurement exhibits a strong correction to scaling: $z=1.60(1)$ ($c_1=1.10$) and one

TABLE I. Independent growth exponent estimates of the d-mer model in different dimensions.

d	α	β	z
2	0.395(5)	0.245(5)	1.58(10)
3	0.29(1)	0.184(5)	1.60(10)
4	0.245(5)	0.15(1)	1.91(10)
5	0.22(1)	0.115(5)	1.95(15)

cannot differentiate it from the $2+1$ dimensional results within the error margins.

In *four spatial dimensions* our best fit for the growth exponent is $b_1=1.08$ and $\beta=0.15(1)$. In the literature $\beta=0.16(1)$ [24] and $\beta=0.146(1)$ [26] values are reported. For the width saturation values the linear fitting results in $\alpha=0.245(5)$ with $a_1=0.07$. This compares with the literature values $\alpha=0.245(1)$ [25] and $\alpha=0.255(5)$ [26]. The z_{eff} seems to converge to $z=1.91(10)$ (with $c_1=-0.64$) but the fluctuations are very strong and we could not reach saturation for sizes larger than $L=128$. Going further by a factor of two in system sizes would require simulations with 8 GB memory and very long CPU times. Our results do not support the field theoretical prediction of $d_c=4$ because we do not observe the disappearance of power-law growth.

In *five dimensions* the local slopes suggest $b_1=0.134$ and $\beta=0.115(5)$ in agreement with $\beta=0.11(1)$ [25] reported for smaller sizes. One can find strong oscillations before the saturation regime. Again these are due to kinematic transport waves in finite system. Initially for $L=64$ we saw a definite increase in β_{eff} as $1/t<0.005$ before the saturation, but this proved to be an artifact of the MT random number generator. When we used different, pseudorandom number generators: drand48 [43] or random( ) of LANGUAGE C, the growth tendency for very late times was much weaker. We think that the site selection, the only source of randomness in case of $p=1$ might not be completely uniform among the 2^{30} possible places. To confirm this we repeated the $5d$ simulations using $p=0.9$ with the MT generator and found agreement with the results using drand48. For the saturation we estimate $\alpha=0.22(1)$ with $a_1=0.08$ and $z=1.95(15)$ with $c_1=-0.55$.

In conclusion we have shown that the mapping of a KPZ surface growth model onto driven lattice gases (DLGs) can be extended to higher dimensions. Although the growth of the surfaces exhibits the spatial symmetry of the underlying lattice, one can map it onto an anisotropic DLG of more complex objects. The coarse grained, continuum description of these d-mers is an anisotropic Burgers equation. Still the DLG model is nontrivial because it is just an oriented drift of d-mers with hardcore exclusions. The topological constraint is the consequence of the required surface continuity by the mapping. In two dimensions we confirmed [37] that the probability distribution $P(W^2)$ matches the universal scaling function determined for another KPZ model [27]. We presented effective bit-coding simulations and high precision results for the exponents α, β, and z independently (see

Table I). The sensitive local slope analysis provides numerical agreement with former simulation results but for larger sizes, which have not been investigated so far, we see a slight growing tendency in the β_{eff} exponents in all dimensions. For $d=2$ our results marginally overlap with the $\beta=1/4$ value suggested some time ago by RG. The change toward a trivial behavior in higher dimensions in the DLG language would mean the disappearance of the topological constraints among the extended d-mer objects as they could follow a simple ASEP dynamics of point particles. This will be the target of further studies using massively parallel algorithms on graphic cards. We hope that we will be able to obtain a firm estimate for the upper critical dimension using extrapolation techniques.

---

[1] M. Kardar, G. Parisi, and Y. C. Zhang, Phys. Rev. Lett. **56**, 889 (1986).

[2] J. M. Burgers, *The Nonlinear Diffusion Equation* (Riedel, Boston, 1974).

[3] D. Forster, D. R. Nelson, and M. J. Stephen, Phys. Rev. A **16**, 732 (1977).

[4] A. L. Barabási and H. E. Stanley, *Fractal Concepts in Surface Growth* (Cambridge University Press, Cambridge, 1995).

[5] T. Halpin-Healy and Y.-C. Zhang, Phys. Rep. **254**, 215 (1995).

[6] J. Krug, Adv. Phys. **46**, 139 (1997).

[7] M. Kardar, Phys. Rev. Lett. **55**, 2923 (1985).

[8] H. K. Janssen and B. Schmittmann, Z. Phys. B **63**, 517 (1986).

[9] H. van Beijeren, R. Kutner, and H. Spohn, Phys. Rev. Lett. **54**, 2026 (1985).

[10] T. Hwa, Phys. Rev. Lett. **69**, 1552 (1992).

[11] M. Kardar, Nucl. Phys. B **290**, 582 (1987).

[12] S. F. Edwards and D. R. Wilkinson, Proc. R. Soc. London, Ser. A **381**, 17 (1982).

[13] C. A. Doty and J. M. Kosterlitz, Phys. Rev. Lett. **69**, 1979 (1992).

[14] E. Frey and U. C. Täuber, Phys. Rev. E **50**, 1024 (1994).

[15] M. Lässig, Nucl. Phys. B **448**, 559 (1995).

[16] T. Halpin-Healy, Phys. Rev. A **42**, 711 (1990).

[17] M. Lässig, Phys. Rev. Lett. **80**, 2366 (1998).

[18] S. Stepanow, Phys. Rev. E **55**, R4853 (1997).

[19] J. K. Bhattacharjee, J. Phys. A **31**, L93 (1998).

[20] H. C. Fogedby, Phys. Rev. Lett. **94**, 195702 (2005).

[21] M. Lässig and H. Kinzelbach, Phys. Rev. Lett. **78**, 903 (1997).

[22] M. A. Moore, T. Blum, J. P. Doherty, M. Marsili, J.-P. Bouchaud, and P. Claudin, Phys. Rev. Lett. **74**, 4257 (1995).

[23] L. Canet, H. Chate, B. Delamotte, and N. Wschebor, e-print arXiv:0905.1025.

[24] T. Ala-Nissila, Phys. Rev. Lett. **80**, 887 (1998).

[25] T. Ala-Nissila, T. Hjelt, J. M. Kosterlitz, and O. Venäläinen, J. Stat. Phys. **72**, 207 (1993).

[26] E. Marinari, A. Pagnani, and G. Parisi, J. Phys. A **33**, 8181 (2000).

[27] E. Marinari, A. Pagnani, G. Parisi, and Z. Rácz, Phys. Rev. E **65**, 026136 (2002).

[28] H. Hinrichsen and G. Ódor, Phys. Rev. Lett. **82**, 1205 (1999).

[29] G. Ódor, Rev. Mod. Phys. **76**, 663 (2004).

[30] P. Meakin, P. Ramanlal, L. M. Sander, and R. C. Ball, Phys. Rev. A **34**, 5091 (1986).

[31] M. Plischke, Z. Rácz, and D. Liu, Phys. Rev. B **35**, 3485 (1987).

[32] G. Ódor, B. Liedke, and K.-H. Heinig, Phys. Rev. E **79**, 021125 (2009).

[33] T. Ligget, *Interacting Particle Systems* (Springer-Verlag, Berlin, 1985).

[34] S. Katz, J. L. Lebowitz, and H. Spohn, J. Stat. Phys. **34**, 497 (1984).

[35] B. Schmittman and R. K. P. Zia, in *Phase Transitions and Critical Phenomena*, edited by C. Domb and J. L. Lebowitz (Academic Press, London, 1996), Vol. 17.

[36] M. Matsumoto, M. Saito, H. Haramoto, and T. Nishimura, J. Univers. Comput. Sci. **12**, 672 (2006).

[37] G. Ódor, B. Liedke, and K. Heinig, e-print arXiv:0912.1755.

[38] L. H. Tang, B. M. Forrest, and D. E. Wolf, Phys. Rev. A **45**, 7162 (1992).

[39] F. Family and T. Vicsek, J. Phys. A **18**, L75 (1985).

[40] F. D. A. Aarão Reis, Phys. Rev. E **69**, 021610 (2004).

[41] S.-V. Ghaisas, Phys. Rev. E **73**, 022601 (2006).

[42] S. Gupta, S. N. Majumdar, C. Godréche, and M. Barma, Phys. Rev. E **76**, 021112 (2007).

[43] See, for example, http://linux.die.net/man/3/drand48